Monolithic Dual-Polarized Leaky-Wave Array with Off-Axis Pointing, 36 dBi Gain and Unbalanced Beamforming Networks for Radar Applications

Valentin Lourenço Martins, Erwan Rahault, Aurélie Dorlé, Stéphane Méric, Esteban Menargues, María García Vigueras

Monolithic Dual-Polarized Leaky-Wave Array with Off-Axis Pointing, 36 dBi Gain and Unbalanced Beamforming Networks for Radar Applications

Valentin Lourenço Martins[#$], Erwan Rahault[$], Aurélie Dorlé[#], Stéphane Méric[$],
Esteban Menargues[*], María García Vigueras[$]

[#]DEMR, ONERA, Université de Toulouse, France
[$]Univ. Rennes, INSA Rennes, CNRS, IETR- UMR 6164, France
[*]SWISSto12, Switzerland
valentin.lourenco_martins@onera.fr, maria.garcia-vigueras@insa-rennes.fr

***Abstract* — This paper proposes a compact, lightweight radiating panel for polarimetric radar, consisting of 32 dual-mode leaky waveguides fed by orthomode transducers and unbalanced beamforming networks. The array generates a high-gain pencil beam ($46\,\lambda$ long) with low sidelobes, achieved through equi-phase non-uniform excitation and modulation of the waveguide perforations. The three-layer monolithic panel, 3D printed using selective laser melting, integrates two beamforming networks and the radiating elements. The prototype is well matched for both polarization, it presents high isolation and a high-gain beam with off-axis pointing. This work demonstrates the first monolithic large radiating aperture with such a performance, providing a solution for balancing compactness and complexity in high-gain antenna arrays.**

***Keywords* — High gain, low profile, dual polarization, additive manufacturing.**

I. Introduction

Polarimetric radars use antennas that transmit and receive two independently polarized beams with high isolation. This is especially useful in environments like clouds, forests, ice packs, and oceans, where backscattering is influenced by surface roughness, material composition, and anisotropic features, leading to distinct polarization responses that provide valuable target information. Some missions, such as SWOT [1] and DopplerScatt [2], require off-axis pointing in a monostatic configuration for optimal target retrieval. SWOT uses a dual-polarized Ka-band interferometer with two reflectarrays, one for each polarization [3]. Similarly, DopplerScatt employs a mechanically rotated parabolic reflector with a dual-polarized feed for off-axis pointing, used to retrieve ocean surface currents and wind vectors. In both systems, the antennas are externally fed, resulting in a design that does not meet low-profile requirements due to their volume. Alternatives to mechanical steering involve phased arrays, which enable electronic beam steering but significantly increase antenna complexity and cost. Examples include the Sentinel-1 and RADARSAT Constellation [4], [5].

This paper presents a low-profile antenna solution that eliminates the need for separate radiating panels for each polarization, making it ideal for small platforms like drones or aircraft where compactness is crucial. The antenna uses an array of dual-mode leaky waveguides, excited by an orthomode transducer, to provide dual polarization and off-axis pointing by operating above the cutoff of both fundamental modes [6], [7]. While less flexible than phased arrays, it offers reduced complexity and cost, making it highly competitive for applications where beam scanning is not required at a fixed frequency. The use of waveguide technology enables full-metal implementation through additive manufacturing (AM), ensuring high radiation efficiency, which is critical for autonomous platforms and operation in demanding environments, while minimizing the radiating aperture size to meet performance requirements [8].

While the one-dimensional (1D) radiating element, electrically long along one direction, has been previously demonstrated by some authors [6], [7], its arrangement in a monolithic array has not yet been proven. The implementation of a large bidimensional radiating aperture represents a major step forward, presenting challenges in the design of beamforming networks and enabling monolithic vertical metal printing. This paper demonstrates a grouping of 32 1D elements that occupy a significantly low volume, as the beamforming networks (BFN) for each polarization are folded below the radiating aperture. The feeding of the 32 elements is achieved using an unbalanced BFN that reduces side-lobe level in the azimuthal plane (SLL), resulting in two overlapping pencil beams with orthogonal linear polarizations and excellent isolation between them.

SLL is an essential metric in radar systems which governs the magnitude of parasite echos observed during radar acquisition. The antenna designer must then propose an antenna with the lowest achievable SLL while taking into account the trade-off between SLL, gain, and beamwidth. Various BNFs for low SLL have been proposed in the literature, including a 1:8 Ku-band wideband unequal power divider in SIW with phase error reduction [9], a fully metallic 1:16 power divider fabricated by AM [10], and a dual-polarized, unbalanced power distribution feeding network in gap waveguide technology [11]. To the best of the authors' knowledge, while monolithic high-gain antennas are emerging [12], no other prototype achieves such high directivity,

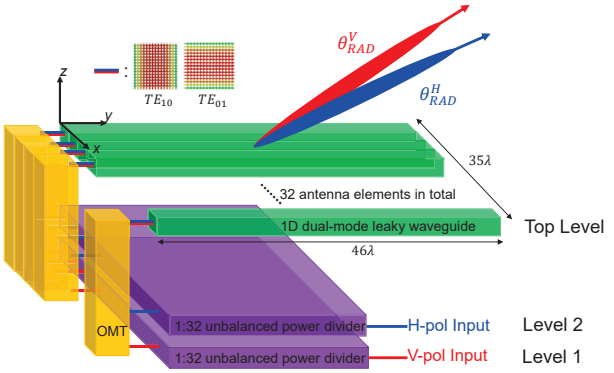

Fig. 1. Schema of array architecture, including leaky-waveguides, OMTs and BFNs.

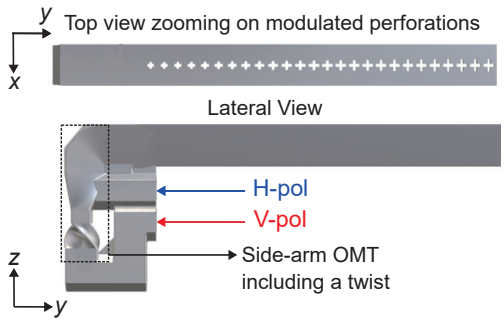

Fig. 2. Detail of the 1D leaky waveguide: (a) zoom of the aperture, (b) side view with OMT and twist.

exceeding existing designs by at least 2 dBi (see [12]). Though some prior works use multilayer architectures, they are simpler, single-polarized, and lack dual-mode waveguides. This paper presents a novel three-level monolithic structure with stacked BFNs feeding the array. To ensure self-support, unconventional waveguides with hexagonal and pentagonal cross-sections are employed, representing an additional innovation.

The concept proposed here is experimentally validated through a fabricated and measured prototype operating in Ka-band, which will be part of the radar instrument for water monitoring HOMARDS that is under development in the IETR laboratory [13]. Weighing under 1 kg with a footprint of 39 cm × 29 cm, the structure offers high compactness and low weight. Measured performance includes a return loss below -10 dB, excellent polarization isolation (> 40 dB), and 36 dBi pencil beams with an off-axis pointing at 52 degrees. This manuscript is organized as follows. Section II describes the structure of the proposed antenna and the design of the BFNs. Section III presents the experimental validation of the manufactured prototype. Conclusions follow in Section IV.

II. Antenna Design

The overall antenna architecture is sketched in Fig. 1, including 32 leaky waveguides fed each of them by OMTs, which combine the dual-polarized signals created by two BFNs (one per polarization). The antenna operates in the Ka-band

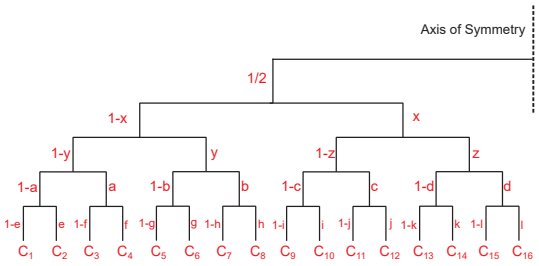

Fig. 3. BFN unbalanced power distribution and definition of ratios and coefficients.

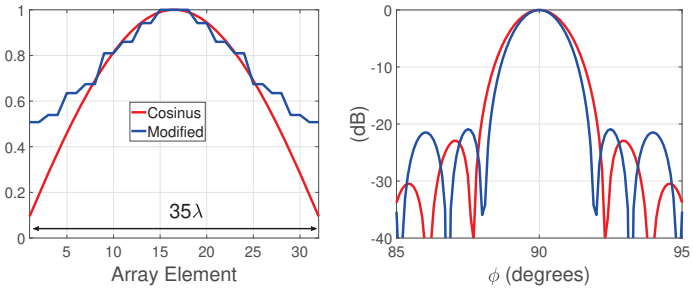

Fig. 4. Normalized distribution : (a) aperture illumination amplitude; (b) Associated array factor.

(centered at 37 GHz) and the following subsections provide details on each of the components.

A. 1D Radiating Element

The radiating element is illustrated in Fig. 2, and it consists of a dual-mode leaky waveguide that supports two fundamental degenerate modes (namely TE_{10} and TE_{01}). Including dual-polarized perforations on the top wall of the waveguide, radiation is induced from both modes simultaneously, thus generating two orthogonally polarized beams from the same aperture. The antenna includes a septum OMT and a twist, in order to excite both modes of the leaky waveguide. Such an antenna element was proposed and validated in [6], showing that excellent cross-polarization and isolation levels can be achieved as long as the design respects the symmetry plane of the waveguide. The size of the perforations is modulated along the propagation axis of the waveguide (see Fig. 2), to reduce the SLLs for both polarizations in the elevation plane [7].

B. Unbalanced power distribution

To feed 32 antennas, a non-uniform amplitude distribution is chosen to pursue -20 dB of SLL. The followed methodology consists in calculating the coefficients of each division stage in the BFN then obtain the associated power ratios [9]. If the divider has 2N outputs and the distribution is symmetric, then there are (N-1) ratios to calculate. Figure 3 shows all the ratios for the unbalanced power divider with the final amplitude coefficients (denoted by $c_1, c_2, \ldots, c_{N/2}$). Note that in order to avoid redundancy, due to BFN symmetry, only half of the structure is shown.

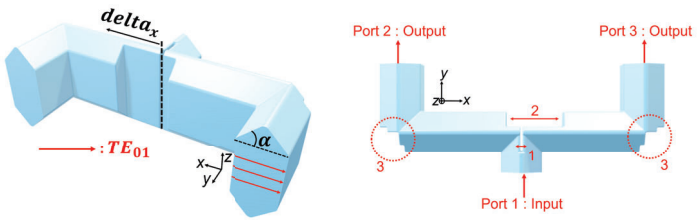

(a) (b)

Fig. 5. Vacuum model of unbalanced power divider: (a) 3D and (b) top view.

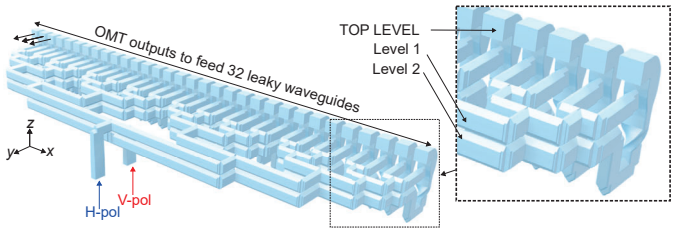

Fig. 6. Vacuum model of the complete 3-level structure integrating 2 BFNs.

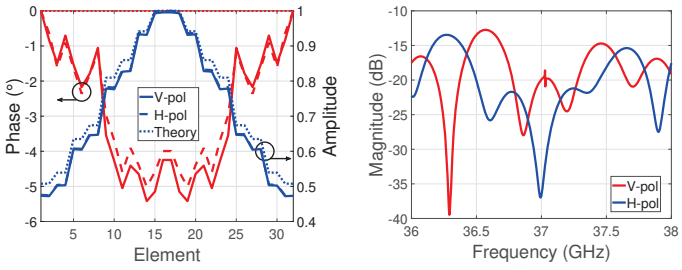

(a) (b)

Fig. 7. BFN Performance : (a) power Distribution ; (b) return Loss.

Given the objective of achieving a 1:32 splitter, it is necessary to implement five stages comprising fifteen distinct power ratios. For the sake of simplicity, the design process has considered a non-canonical power distribution with a progressive shape that meets the SLL specifications while reducing the number of stages required for the design. Thus, the power ratios in Fig. 3 (denoted by $x, y, z, a, b, \ldots, k, l$) have been adjusted in order to reach the desired pattern shape on the array factor. This strategy enables reducing the number of different unequal power ratios to 4.

The resulting values of the power ratios are $x = 0.7, \quad y = 0.61, \quad z = 0.575, \quad a, b, c, d = 0.53, \quad e, f, g, h, i, j, k, l = 0.5$. The corresponding amplitude distribution and associated array factor can be seen in Fig. 4. This figure shows that the resulting illumination approaches a cosine distribution and the SLL in the array factor remains well below -20 dB.

C. Implementation of BFN Power Ratios with T-junctions

Different topologies of power divider have to be found in order to implement the previously computed power ratios. The generic T-junction topology of Fig. 5 is selected for the sake of compactness. As the figure shows, the waveguide sections that are employed are characterized by non-conventional cross-sections. These geometries have been chosen to enable monolithic 3D-print of the piece without undesired supports. As it is explained in [14], a certain inclination angle α has to be considered.

The splitter, with one input and two outputs, divides power with minimal loss and equal phase delay. Its components are shown in Fig. 5b: "1" separates the guided wave, "2" adjusts the power ratio by translating the gap along the x-axis, and "3" matches impedance to reduce reflections.

As illustrated in Fig. 5a, adjusting the ratio via translation introduces a phase shift, increasing with imbalance. To compensate for this and preserve the radiation pattern, arm lengths were adjusted. Five stages were designed, achieving the required ratios with excellent matching (S_{11} < -30 dB) and minimal phase error.

D. Complete Beamforming Network

The vacuum model of the complete BFN can be seen in Fig. 6, and its associated performance is given in Fig. 7. It can be seen that the BFN has a return loss level below -20 dB in the band of interest (from 36.84 to 37.16 GHz) and below -10 dB between 36 and 38 GHz. The difference that it is observed between the return losses obtained for the two polarizations can be explained by the 1-plane symmetry of the side-arm OMT. Figure 7b shows that the distributions (amplitude and phase) are very close for the two polarizations and very similar to the one predicted in the previous section.

III. Experimental Validation

The proposed concept is validated through the fabrication of a prototype using selective laser melting (SLM) in an aluminum alloy by the company SWISSto12 [14]. The number of radiating elements in the array is selected to achieve a realized gain greater than 35 dBi. The prototype has dimensions of $39\,\text{cm} \times 29\,\text{cm} \times 6\,\text{cm}$. To the best of the authors' knowledge, this is the monolithic 3D-printed device with bigger radiating aperture in the literature [12]. Additionally, the complexity of the prototype is notable, as it integrates perforated waveguides, OMTs, twists, and T-junctions within a 3-layer structure. It is important to emphasize that if traditional subtractive manufacturing methods were used, the weight would be significantly higher.

Photographs of the prototype are shown in Fig. 8, with views from the top (radiating aperture) and back (showing the input ports and four cylindrical support columns). Details of the three-layer monolithic structure and power dividers are shown in Figs. 8c and 8d. The BFN includes small non-radiating holes for depowdering.

The prototype is currently being measured at IETR and ONERA. The matching and isolation of the two input ports are shown in Fig. 9a, with measured results aligning well with simulations. Between 36 GHz and 38 GHz, the matching for both polarizations remains below $-10\,\text{dB}$, while isolation stays below $-40\,\text{dB}$. The realized gain in the azimuthal plane is presented in Fig. 9b, showing a main beam gain of approximately 37 dBi at 37 GHz (37.25 dBi for H-pol

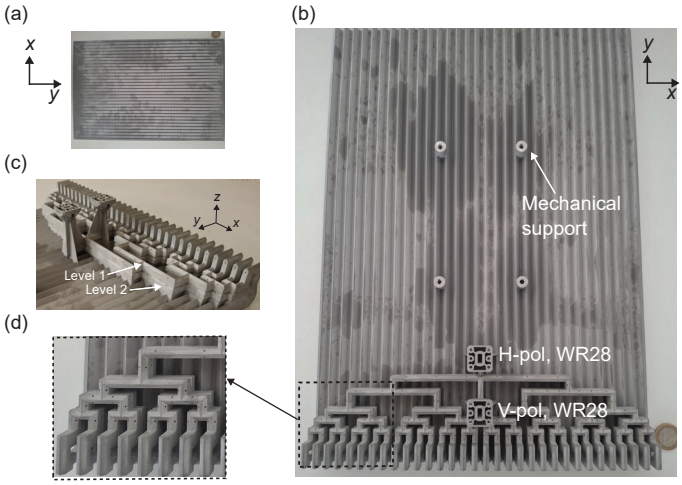

Fig. 8. Several views of the printed antenna with a detailed view of the BFN; (a) Top view: Radiating aperture; (b) Back view: Beamforming Network; (c) Back view: layers 1 and 2; (d) Back view: zoom on the BFN.

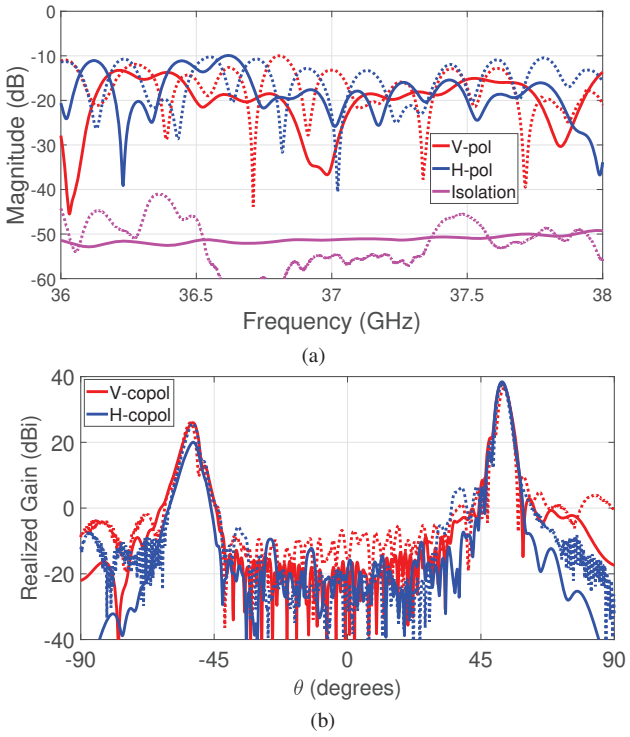

Fig. 9. Experimental results (continuous/dotted lines correspond respectively to full-wave simulations/ measurements). (a) Input ports matching and isolation; (b) Co-pol azimuth pattern measured at 37 GHz.

and 36.43 dBi for V-pol), which aligns perfectly with the expectations. Both beams point around 52°, with a pointing angle difference $\theta^V_{RAD} - \theta^H_{RAD}$ below 0.8°.

IV. Conclusion

This paper presents a monolithically built, full-metal dual-polarized radiating panel designed as a 32-element array with two beamforming networks (BFNs) in a compact 3-layer structure. The BFNs utilize unbalanced power dividers to minimize sidelobe levels (SLLs) and incorporate non-canonical waveguides. Experimental validation confirms very good agreement with simulations, demonstrating the panel's potential for energy-efficient, small airborne radar systems.

Acknowledgment

The authors thank Loïc Castanet (ONERA) and Alban Mourier (SWISSto12) for their valuable help in the experimental campaign. This work was supported by the French Ministry of Defence (AID), ONERA, the Ministry of Higher Education and Research, Rennes Métropole and Conseil Départemental 35 (CPER SOPHIE / STIC & Ondes), as well as the European Union (ERDF funds).

References

[1] P. Vaze, S. Kaki, D. Limonadi, D. Esteban-Fernandez, and G. Zohar, "The surface water and ocean topography mission," in *2018 IEEE Aerospace Conference*, 2018, pp. 1–9.

[2] E. Rodríguez, A. Wineteer, D. Perkovic-Martin, *et al.*, "Ocean surface currents and winds using dopplerscatt," in *IGARSS 2018 - 2018 IEEE International Geoscience and Remote Sensing Symposium*, 2018, pp. 1474–1476.

[3] E. Peral, D. Esteban-Fernández, E. Rodríguez, *et al.*, "Karin, the ka-band radar interferometer of the swot mission: Design and in-flight performance," *IEEE Transactions on Geoscience and Remote Sensing*, vol. 62, pp. 1–27, 2024.

[4] E. S. Agency, *Sentinel-1 mission*, https://sentinels.copernicus.eu/web/sentinel/missions/sentinel-1, 2023.

[5] C. S. Agency, *Radarsat constellation mission (rcm)*, https://www.asc-csa.gc.ca/eng/satellites/radarsat/default.asp, 2023.

[6] M. García-Vigueras, E. Menargues, T. Debogovic, E. de Rijk, and J. R. Mosig, "Cost-effective dual-polarised leaky-wave antennas enabled by three-dimensional printing," *IET Microwaves, Antennas & Propagation*, vol. 11, no. 14, 1985-1991, 2017.

[7] A. Dorlé, R. Gillard, E. Menargues, *et al.*, "Additive manufacturing of modulated triple-ridge leaky-wave antenna," *IEEE Antennas and Wireless Propagation Letters*, vol. 17, no. 11, pp. 2123–2127, 2018.

[8] D. Pla, S. Capdevila, A. Calleau, *et al.*, "High efficiency and circular polarization in satcom phased arrays using tri-ridge apertures," in *Scientific Reports*, 2024.

[9] S. S. Hasan, F. Jiewei, K. Nemai, A. E. Md, and W. Jeffrey, "Improved wideband phase balancing siw unequal power divider design for the low side-lobe array antennas," *IET Microwaves, Antennas & Propagation*, vol. 15, no. 2, pp. 115–122, 2021.

[10] G.-L. Huang, C.-Z. Han, W. Xu, T. Yuan, and X. Zhang, "A compact 16-way high-power combiner implemented via 3-d metal printing technique for advanced radio-frequency electronics system applications," *IEEE Transactions on Industrial Electronics*, vol. 66, no. 6, pp. 4767–4776, 2019.

[11] X. Cheng, X. Chen, J. Liu, *et al.*, "Compact dual-polarized low sidelobe monopulse slot antenna array based on gap waveguide technology," *IEEE Transactions on Antennas and Propagation*, pp. 1–1, 2024.

[12] S. Wu, J. Li, J. Yao, Y. Cao, Y. Li, and X. Y. Zhang, "3-d-printed ka-band circularly polarized monopulse antenna array with high gain and low axial ratio," 11, vol. 72, 2024, pp. 8282–8293.

[13] E. Rahault, S. Méric, M. García-Vigueras, *et al.*, "Homards: An airborne ka-band radar sensor for supporting future satellite missions," in *2023 20th European Radar Conference (EuRAD)*, 2023, pp. 189–192.

[14] M. García-Vigueras, L. Polo-Lopez, C. Stoumpos, A. Dorlé, C. Molero, and R. Gillard, "Metal 3d-printing of waveguide components and antennas: Guidelines and new perspectives," in *Hybrid Planar*, M. D. Fernandez, J. A. Ballesteros, H. Esteban, and Ángel Belenguer, Eds., Rijeka: IntechOpen, 2022, ch. 6.